Article
Vol. 23, No. 6, p. 881–894, December 2019
https://doi.org/10.1007/s12303-019-0010-2
pISSN 1226-4806 eISSN 1598-7477
Geosciences Journal GJ

Quartz OSL dating of palaeosols intercalated with basaltic lava flows and scoria deposits from monogenetic volcanoes in northeastern Jeju Island, Korea

Eun-Young Yeo[1,2], Jeong-Heon Choi[2]*, Ung San Ahn[3], and Albert Chang-sik Cheong[1,2]

[1]Graduate School of Analytical Science and Technology, Chungnam National University, Daejeon 34134, Republic of Korea
[2]Division of Earth and Environmental Sciences, Korea Basic Science Institute, Chungbuk 28119, Republic of Korea
[3]World Heritage Office, Jeju Special Self-Governing Provincial Government, Jeju 63341, Republic of Korea

ABSTARCT: Jeju Island, which lies on the continental shelf in the southern Korean Peninsula, is the emergent portion of a basaltic volcanic field that has erupted since the Early Pleistocene (ca. 1.8 Ma). Volcanic activity that continued into historic times (ca. 1 ka) formed an elongated shield with a central edifice (Mt. Halla) and more than 300 monogenetic cones and rings. The establishment of a temporal framework for Jeju volcanism, particularly during the Late Pleistocene and Holocene activities, requires geochronological tools other than radiometric dating techniques, which are based on parent-daughter isotope pairs with geologically long half-lives, such as $^{40}Ar/^{39}Ar$ dating. In this study, we conducted quartz optically stimulated luminescence (OSL) dating of palaeosols intercalated with basaltic lava flows and scoria deposits, presumably ejected from three monogenetic volcanoes (Cheoreum, Darangsh and Dunjibong volcanoes) in the northeastern part of the island. Quartz extracts from the palaeosols had moderate to dim sensitivity to optical stimulation, but several prerequisite tests of the measurement protocols for equivalent dose estimation were successful. The coarse (63–250 μm) and fine (4–11 μm) quartz fractions yielded continuous wave (CW)-OSL ages of 19.9–7.0 and 18.6–6.7 ka, respectively, both of which were broadly consistent with the radiocarbon dates (10245–7440 Cal yr BP). These ages indicate that lava flows and scoria deposits covering the palaeosols are younger than ~7 ka. The pulsed OSL signals in coarse quartz extracts from the palaeosols suffered from poor counting statistics, thus it is recommended that they not be applied solely (i.e., without any other absolute ages to compare) to dating dim samples. From one of the sites investigated here, the averaged sedimentation rate of the palaeosol is estimated to be ~0.05 mm/yr, based on stratigraphically consistent CW-OSL ages. The OSL ages presented in this paper, together with previous OSL and radiocarbon ages, confirm that Jeju volcanic island was regionally active during the Holocene.

Key words: Jeju Island, monogenetic volcanoes, palaeosol, OSL, Holocene

Manuscript received December 27, 2018; Manuscript accepted March 1, 2019

1. INTRODUCTION

Recent advances in luminescence dating method have considerably expanded its applicability in terms of datable age range (e.g., Thiel et al., 2012; Li et al., 2013; Sun et al., 2017) and materials to be dated (e.g., Sohbati et al., 2015; Jenkins et al., 2018; Gliganic et al., 2019). However, establishing a geochronology of volcanic rocks and related sediments using luminescence dating methods remains challenging, mainly due to the lack of dosimeter minerals, quartz and K-rich feldspars. Even where quartz and feldspars exist in volcanic materials, they have been reported to show various undesirable luminescence characteristics for reliable dating; for instance, since earlier, it has been observed that luminescence signals in "volcanic quartz" are dominated by non-fast optically stimulated luminescence (OSL) components (Tsukamoto et al., 2003; Choi et al., 2006), which may result in significant OSL age underestimation (Bonde et al., 2001). Tsukamoto et al. (2011) have performed intensive works to assess the possibility of luminescence dating of basaltic rocks that contain plagioclase feldspars. Despite their success in dating young basaltic rocks after correcting for anomalous fading (~10–14 ka), the reports

*Corresponding author:
Jeong-Heon Choi
Division of Earth and Environmental Sciences, Korea Basic Science Institute, 162 Yeongudanji-ro, Cheongwon-gu, Cheongju, Chungbuk 28119, Republic of Korea
Tel: +82-43-240-5333, Fax: +82-43-240-5179, E-mail: jhchoi@kbsi.re.kr

on luminescence dating of volcanic rocks have been rare since then.

To some extent, these difficulties in dating volcanic rocks using luminescence techniques have limited the establishment of a geochronology of volcanic activities on Jeju Island (a volcanic island located on the continental shelf ~90 km off the southern coast of the Korean Peninsula), particularly for events during the Late Pleistocene and the Holocene. This island consists of more than 300 monogenetic volcanoes; thus, providing the reliable ages of these volcanoes is essential to reconstruct its eruption history. Conventional radiometric dating of these young volcanoes using isotope pairs with long half-lives poses many challenges, mainly due to the small amount of radiogenic daughter isotopes. In the case of ^{40}Ar-^{39}Ar dating, problems associated with excess argon invalidate the accurate dating of young volcanoes (e.g., Esser et al., 1997; Ramos et al., 2016).

Recently, instead of dating volcanic rocks directly, a few attempts have been made to date sediments under- or overlying lava flows from several localities encompassing the whole Jeju Island, using OSL and radiocarbon dating methods (see Fig. 1a

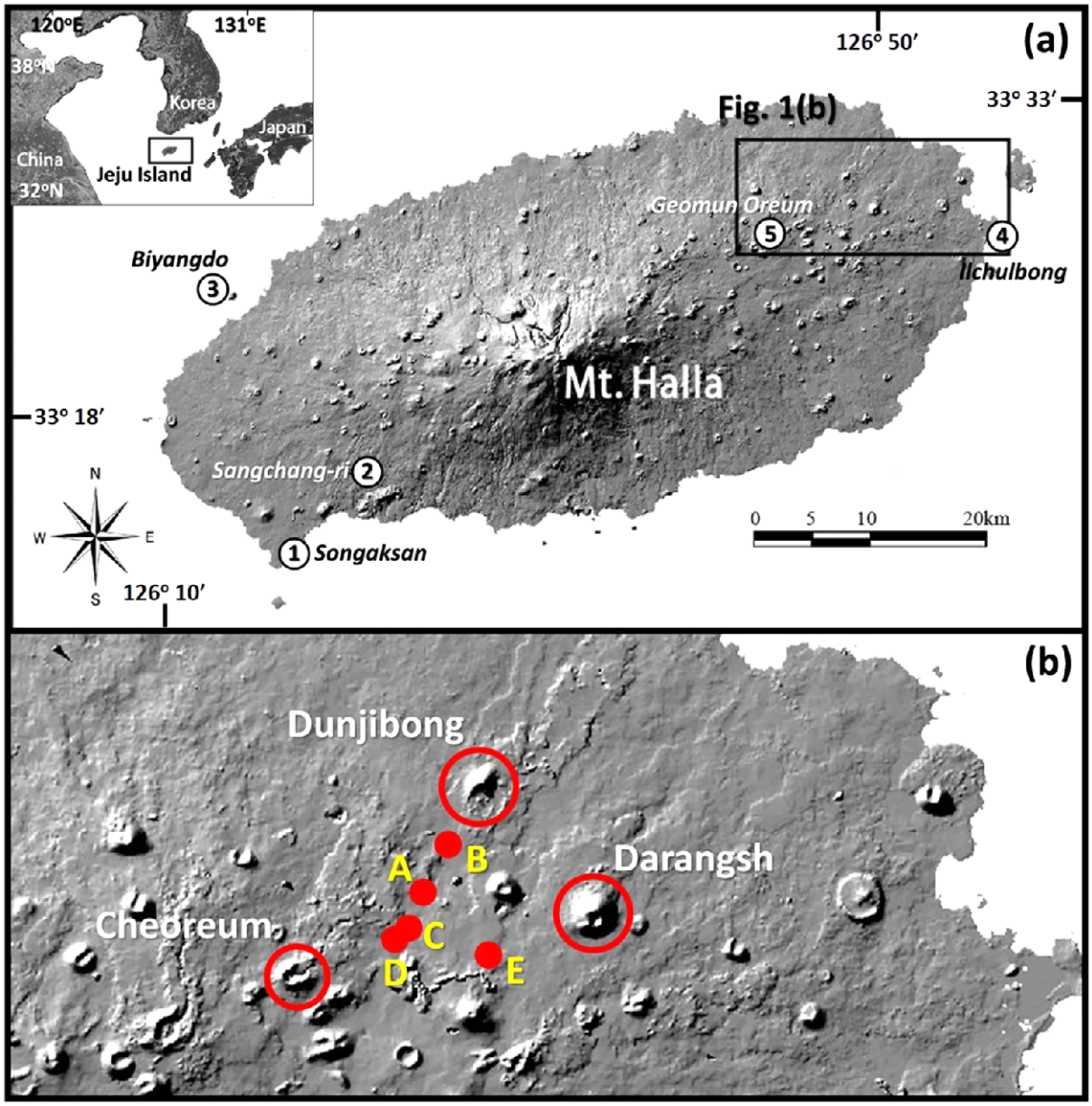

Fig. 1. The study area and sampling sites. (a) Numbers indicate the locations of the previously dated sites. The site names, ages, dating methods and the references are; 1. Songaksan (~4000 yr BP, ^{14}C, Sohn et al., 2002; 5–7 ka, OSL, Cheong et al., 2007; < 3.8 ka, OSL, Ahn, 2016), 2. Sangchang-ri (< 5 ka, ^{14}C and OSL, Lee et al., 2014), 3. Biyangdo (> 4.5 ka, ^{14}C, Ahn, 2016), 4. Ilchulbong (< 6–7 ka, ^{14}C and OSL, Ahn, 2016), 5. Geomun Oreum (< 8 ka, ^{14}C and OSL, Ahn et al., 2017). (b) 18 palaeosol samples were taken from 5 sites (Sites A, B, C, D and E; solid circles in red), where the palaeosols are intercalated with lava flows and scoria deposits, ejected from three monogenetic volcanoes, Cheoreum, Darangsh and Dunjibong.

for the locations of previous investigations). Lee et al. (2014) reported OSL and radiocarbon ages of ~5 ka from the sediments beneath lava formations in Sangchang-ri, and argued that Jeju Island has been volcanically active until very recently. Ahn (2016) constrained the eruption timing of monogenetic volcanoes in Songaksan and Ilchulbong to be younger than 3.8 and 6–7 ka, respectively, and also proposed that Biyangdo erupted before ~4.5 ka using the OSL and radiocarbon ages of sediments intercalating each lava flow. Ahn et al. (2017) used a similar approach to figure out the formation timing of Geomun Oreum and concluded that it erupted after ~8 ka. These ages, together with the earlier dating results by Sohn et al. (2002) and Cheong et al. (2007), suggest that Jeju Island was volcanically active during the Holocene.

While the OSL dating method has been used as an essential tool for dating in previous studies, the OSL signal properties of quartz from palaeosols have not been intensively investigated or described in detail. Furthermore, there have been no investigations of the reliability of the OSL ages of palaeosols intercalated with lava flows on Jeju Island.

In this paper, we investigated the OSL properties of quartz extracts from the palaeosols intercalated with basaltic lava flows and scoria deposits, presumably ejected from three monogenetic volcanoes, Cheoreum, Darangsh and Dunjibong in the northeastern part of Jeju Island. The OSL ages, based on continuous wave (CW)-OSL signals in the coarse and fine quartz fractions, are examined. In addition, we applied pulsed OSL (POSL) dating to palaeosol samples for the first time in Jeju Island, and discussed its reliability in comparison with conventional CW-OSL ages.

2. STUDY AREA AND SAMPLE DETAILS

2.1. Overview of the Formation and Volcanism of Jeju Island

Jeju Island is located ~600 km from the subduction front of the Philippine Sea Plate beneath the Eurasian Plate. Such a long distance from the trench and oceanic island basalt-like geochemistry of erupted rocks has led many investigators to propose a mantle plume origin (e.g., Nakamura et al., 1989; Tatsumi et al., 2005). Alternatively, a tectonic link between subduction processes and intraplate volcanism at Jeju was favoured by more recent geochemical, geochronological, and petrologic studies (Brenna et al., 2012a, 2012b, 2015). The volcanic activity began with dispersed phreatomagmatic eruptions at ~1.8 Ma (Sohn and Park, 2004), and lasted until historic times (Lee and Yang, 2006). Quasi-continuous small-volume volcanism, intercalated with large-volume lava effusion, has resulted in the formation of an elongated shield with a central volcanic edifice (Mt. Halla) and more than 300 monogenetic scoria cones, together with minor tephra rings, maars and lava domes. Three geochemically distinct volcanic stages have been recognized by ^{40}Ar-^{39}Ar dating and elemental/isotopic data from surface rocks and drill cores (Brenna et al., 2012a, 2012b, 2015; Koh et al., 2013). Stage 1 (ca. 1.8 Ma–500 ka) erupted high-Al alkalic basalts and trachytic lavas, whereas Stage 3 (the last 250 ka) produced low-Al alkalic and subalkalic magmas. Geochemically transitional magmas were produced during the intervening Stage 2. The uppermost part of the island (Mt. Halla) consists of latest Pleistocene (~30 ka) trachytes and subsequent basalts (Koh et al., 2003; Ahn and Hong, 2017).

2.2. Study Area and Sampling

There are more than 40 monogenetic volcanoes in the northeastern part of Jeju Island. In this study, palaeosol profiles beneath lava flows and scoria deposits, which are ejected from three monogenetic volcanoes (Cheoreum, Dunjibong, and Darangsh) were chosen for dating.

Cheoreum is a slightly elongated volcano in the southeast direction, with a summit height of ~300 m (a.m.s.l) and a long axis distance of ~0.8 km (Fig. 1b). Erupted lavas from this volcano flowed northeastward, controlled by the original geographic topography. By contrary, lavas from Dunjibong volcano (summit height of ~200 m (a.m.s.l), elongated in an almost north-south direction with a long axis of ~0.5 km), flowed southward and in some places overlies Cheoreum lava flows. Darangsh is a scoria cone, similar in size to Cheoreum volcano. It has a summit height of ~300 m (a.m.s.l) and a long axis distance of ~0.8 km. The scoria ejected from Darangsh can be found as thick layers (~2–3 m) within 2 km from the crater.

At sites A–E (Figs. 1b and 2), age-unknown palaeosols are intercalated with Cheoreum and Dunjibong lava flows and Darangsh scoria deposits. The thickness of the palaeosols at all sites is on a scale of a few tens of centimeters. Within this small scale, the palaeosols were observed to be homogeneous, and we could not find any field evidence of variation in sedimentary features. The samples for OSL dating were collected by inserting light-tight metal tubes (30 cm in length and 4.5 cm in diameter) into palaeosol profiles.

At site A (N33°28′50″/E126°46′56″), a palaeosol layer, pale brown in colour and ~50 cm in thickness, is observed beneath Cheoreum lava flow. Four samples were taken from the palaeosol immediately below the lava (CAS62-1-1, CAS62-2 and CAS62-2-3 for OSL dating, and CAS62-1-C1 for ^{14}C dating) (Fig. 2a). Two other OSL samples (CAS62-1-4 and CAS62-1-5) were also collected in stratigraphic order.

Palaeosols at site B (N33°29′25″/E126°47′21″) are observed beneath Cheoreum lava in the lower part, and between Cheoreum

https://doi.org/10.1007/s12303-019-0010-2

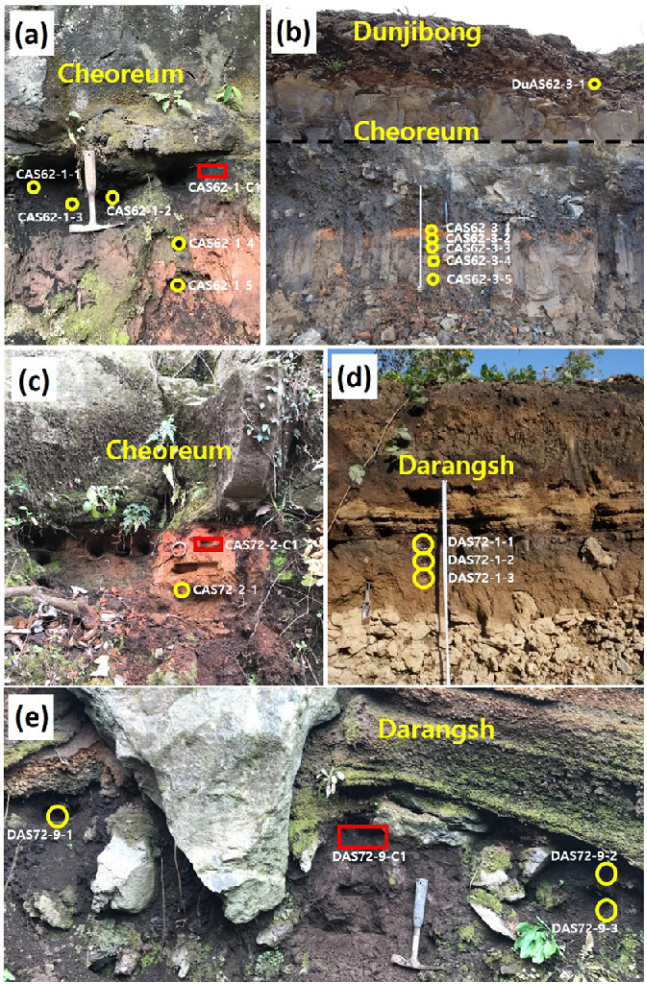

Fig. 2. OSL and ^{14}C samples from the study area (a) Site A, (b) Site B, (c) Site C, (d) Site D and (e) Site E. From sites A–E, eighteen and three palaeosol samples were taken from each profile for OSL and ^{14}C dating, respectively.

and Dunjibong lavas in the upper part (Fig. 2b). From the lower part, five OSL samples were collected from pale brown palaeosols in stratigraphic order (CAS62-3-1, CAS62-3-2, CAS62-3-3, CAS62-3-4 and CAS62-3-5). One OSL sample was collected from a thin (~10 cm) reddish brown palaeosol layer between Cheoreum and Dunjibong lavas (DuAS62-3-1).

At site C (N33°28′26″/E126°46′42″), one palaeosol sample was taken from immediately beneath Cheoreum lava for ^{14}C dating (CAS72-2-C1). Below this, one OSL sample (CAS72-2-1) was also taken (Fig. 2c).

At sites D (N33°38′19″/E126°46′38″) and E (N33°28′5″/E126°47′51″), dark brown palaeosols, ~20–40 cm in thickness, are covered by layered scoria deposits ejected from Darangsh volcano (Figs. 2d and e). Six samples (three samples for each site) were collected for OSL dating (DAS72-1-1, DAS72-1-2, and DAS72-1-3 from site D; DAS72-9-1, DAS72-9-2, and DAS72-9-3 from site E). One sample was collected from site E for ^{14}C dating (DAS72-9-C1).

A total of seven basaltic rocks collected from Cheoreum and Dunjibong lavas at sites A, B and C were analyzed for major element compositions using an X-ray fluorescence at Activation Laboratories (Ontario, Canada). The chemical compositions of the lavas are briefly summarized here for reference. The major element concentrations of the samples were in the range of 47–50 weight % for SiO_2, 14–17% for Al_2O_3, 6–10% for MgO and 4–6% for ($Na_2O + K_2O$). Therefore, the lavas from Cheoreum and Dunjibong volcanoes are classified as basalt or trachy-basalt, and belong to the low-Al alkalic group that mainly erupted during Stage 3 (Brenna et al., 2015 and references therein).

3. SAMPLE PREPARATION, FACILITIES AND METHODS

3.1. OSL Dating

In a subdued dark room in Korea Basic Science Institute (KBSI), coarse fractions were wet sieved from the samples to recover the size fraction of 63–250 μm. Usually, in OSL dating using coarse quartz grains, sample fractions with narrower size intervals (e.g., 90–250 μm, 180–250 μm etc.) are favoured. However, our preliminary test sieving revealed that the sample amount within these narrower intervals was so scarce that we decided to collect the grains in the wider size range of 63–250 μm to ensure a suitable sample amount. According to the data presented in Aitken (1985), this increase in grain size range is not expected to have a critical effect on the evaluation of absorbed doses in quartz.

These coarse fractions were then cleaned with 10% HCl (1 h) and 10% H_2O_2 (~3 h), and etched with conc. HF (1 h), followed by heavy density separation using sodium polytungstate solution (SPT; $2.62 < \rho < 3.00$ g/cm^3) to extract pure quartz grains. Note that, although we chose the broad grain size fraction of 63–250 μm as described above, the amounts of recovered grains from some samples at sites A and B (CAS62-1-4, CAS62-1-5, CAS62-3-2, CAS62-3-3, CAS62-3-4 and CAS62-3-5) were still insufficient for detailed OSL experiments and dating. Thus, for these samples, HF etching was not conducted.

Fine quartz fractions (4–11 μm) of the samples were also prepared for inter-comparison with the OSL ages derived from the coarser counterparts; Fine quartz grains were recovered using Stokes' law of settling, and through routine acid treatments involving 10% HCl (1 h), 10% H_2O_2 (~3 h), and 40% H_2SiF_6 for a week.

After the sample preparation, the purity of coarse and fine quartz extracts was examined, particularly to check whether K-rich feldspars were effectively removed by the sample preparation procedure. Because the presence of K-rich feldspars in quartz extracts may cause several difficulties in equivalent dose and dose rate estimation (Ankjærgaard et al., 2010), it is prudent to

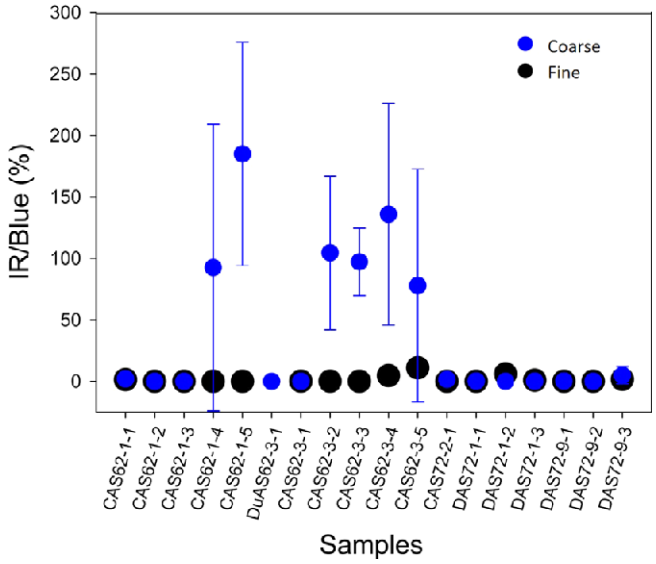

Fig. 3. The ratios of IR to Blue stimulated luminescence signals after sample preparation procedures. The ratios for coarse and fine fractions are depicted by blue and black solid circles, respectively. Six samples, which were not etched with HF due to insufficient amount of coarse quartz, show high IR/Blue ratios over ~80%.

make sure that the K-rich feldspar content is negligible in the quartz extracts. The purity of the samples was checked by observing the response of natural and laboratory irradiated (~20 Gy) aliquots (three aliquots for each sample) to InfraRed (IR) stimulation.

As shown in Figure 3, with the except of six samples (coarse grain) that were not etched with HF due to sample scarcity, IR Stimulated Luminescence (IRSL) signal intensities for most samples were far less than the blue-stimulated signals (< 5%). This implies that K-rich feldspars were effectively removed through the preparation procedure described above, thus will not affect the equivalent dose estimation.

All the quartz OSL signals were read out using a standard Risø reader (Model TL/OSL-DA-20) in KBSI. The reader is equipped with a $^{90}Sr/^{90}Y$ beta source delivering 0.090 ± 0.001 Gy/s (for coarse grains) and 0.080 ± 0.001 Gy/s (for fine grains) to the sample position; Beta source was calibrated using calibration quartz (CAL-Q Batch 99, Risø DTU). Blue-LEDs (470 nm, FWHM = 20 nm, maximum power density of ~80 mW/cm^2) were used for optical stimulation of the samples and the signal detection was through 7 mm Hoya U-340 optical filter. The reader is also equipped with a POSL attachment for the measurement of POSL signals of the samples (see section 4.4. POSL Signal and Dose Recovery Test).

Quartz equivalent doses (D_e's) were estimated using the Single Aliquot Regenerative Dose (SAR) protocol (Murray and Wintle, 2000, 2003). In the following experiments and dating, particularly for the samples which were not etched with HF due to low sample amount, IR washing at 125 °C for 100 s was applied prior to every blue-stimulation in the SAR procedure in order to reduce any effect from K-rich feldspar contamination (double SAR; Roberts, 2007). For the D_e estimation of coarse and fine quartz grains, multiple grain aliquots were used.

The dose rates of the samples were obtained using a low-level high resolution gamma spectrometer installed in KBSI. Alpha efficiency value (a-value) of 0.03 was used to calculate dose rates for fine grains (Mauz et al., 2006).

3.2. ^{14}C Dating

To provide independent age controls for the OSL ages, radiocarbon dating was also performed on three soil samples (CAS62-1-C1, CAS72-2-C1 and DAS72-9-C1) using an Accelerator Mass Spectrometer in Beta Analytic. The conventional radiocarbon ages were calculated using the half-life of 5568 yrs (Libby half-life). The conversion of the conventional radiocarbon ages to calendar years was by using the database INTCAL13 (Reimer et al., 2013) and confidence intervals at the 2σ level were obtained using the High Probability Density Range (HPD) method (Bronk Ramsey, 2009).

4. RESULTS AND DISCUSSION

4.1. Quartz CW-OSL Properties

Before the D_e estimation of the samples, we characterized the quartz CW-OSL shine-down curves for the selected sets of samples. Coarse and fine quartz aliquots from five samples (one sample from each site; CAS62-1-2, CAS62-3-1, CAS72-2-1, DAS72-1-3, and DAS72-9-3) were first preheated at 260 °C for 10 s. Then, the natural quartz CW-OSL signals of each sample were observed at 125 °C for 40 s, with the maximum power density of a stimulation light source (blue-LEDs; ~80 mW·cm^{-2}) (Fig. 4). All of the OSL experiments and dating in this study used "8 mm aliquots" for both size fractions.

This experiment indicated that both coarse and fine quartz grains were not very sensitive to optical stimulation, the initial count rates being in the range of ~100 – ~10000 (cts/0.16 s) (Figs. 4a and b). The OSL signal intensities for most samples were, however, observed to decrease to less than 10% of their initial count rates in 1–2 s after the onset of optical stimulation. As indicated by the fast decay of each shine-down curve, it seems that the OSL signals of the samples are dominated by the fast OSL component, which is the target signal applied to the SAR protocol (Wintle and Murray, 2006). It should be noted here that sample CAS72-2-1 from site C showed most insensitive OSL signals for both coarse and fine fractions, with the initial OSL signal count rates of 100–200 cts/0.16 s. Also, the CW-OSL

https://doi.org/10.1007/s12303-019-0010-2

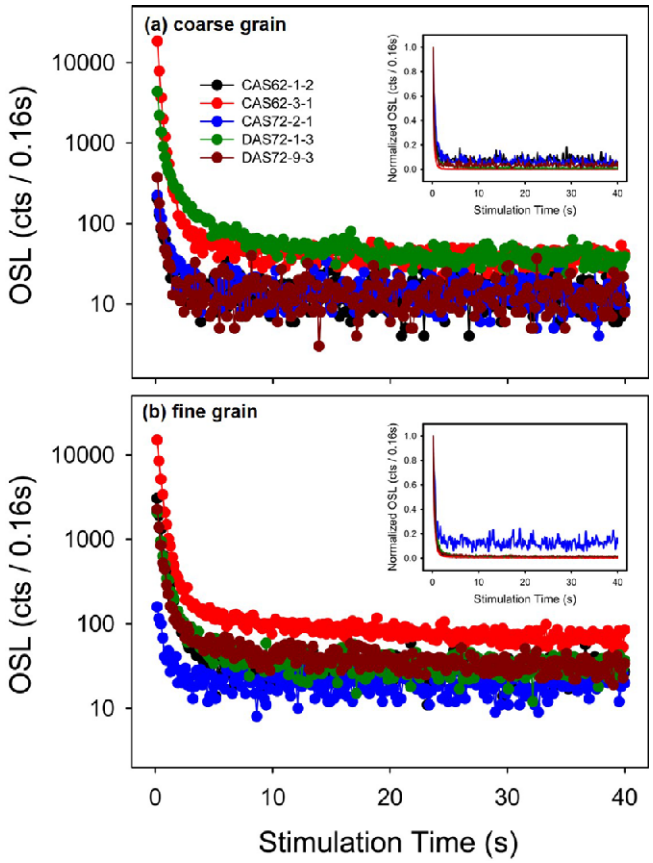

Fig. 4. Continuous-wave (CW) OSL decay curves of natural (a) coarse and (b) fine quartz fractions (one sample from each site) measured at 125 °C for 40 s, after a preheat at 260 °C for 10 s. Except one sample from site C, the initial count rates of most quartz aliquots are ranging ~1000–10000 cts/0.16 s. Normalized CW-OSL signals are shown in the insets for comparison.

decay of this sample was relatively slower than others, reaching 10% of its initial count rates in ~4 s after the onset of optical stimulation (insets to Figs. 4a and b).

4.2. Preheat Plateau Test

When estimating quartz D_e values using the SAR protocol, it is prudent to examine whether the D_e values of the samples are significantly affected by charges that are thermally transferred from light insensitive shallow traps by heating during the measurement procedure. This was tested by performing preheat plateau tests on four representative samples CAS62-3-1, DAS72-1-3, DAS72-9-2, and DAS72-9-3. In this test, 24 aliquots of coarse quartz grains from each sample were prepared and these were preheated from 220 °C to 295 °C (in 15 °C steps), and then held at the raised temperatures for 10 s, cut-heat temperature (i.e., test-dose preheat) being fixed at 220 °C (for 0 s); four aliquots per preheat temperature were used to derive "apparent" D_e values. In addition, at the end of every test dose OSL measurement step during the SAR protocol, the samples were optically bleached for 40 s at the elevated temperatures that were set to be 20 °C higher than the preheat temperatures, in order to minimize the build-up of any slower OSL components (e.g., Murray and Wintle, 2003; Fuchs et al., 2012). As shown in Figure 5, we could not observe any clear dependency of D_e values on preheat temperatures. This implies that, for the samples collected in this study, thermally transferred charges during heating treatment in the SAR protocol do not significantly affect the D_e values of the samples.

4.3. Dose Recovery Test using CW-OSL Signal

As one of the prerequisite tests for reliable D_e estimation, it has now become common practice to examine the ability of a measurement protocol to recover artificial doses administered to samples, which is known as a dose recovery test (Wintle and Murray, 2006).

To check the suitability of the SAR protocol for dating our samples, both coarse and fine quartz grains from all samples (three to six aliquots per sample, depending on the sample amount) were bleached with blue-LEDs for 1000 s twice, with an intervening storage at room temperature for 10000 s to allow charges in the shallow (thermally unstable) traps to thermally decay. After laboratory optical bleaching, known doses (i.e., given doses), the size of which were designed to be similar to the assumed D_e values of each sample, were administered to the samples as natural surrogates using the beta source in the luminescence reader. Then, the SAR protocol was applied to recover the given doses, with preheating at 260 °C for 10 s, cut-heat to 220 °C (for 0 s) and high temperature optical wash at the end of every SAR cycle (at 280 °C for 40 s). These heating conditions were chosen based on the preheat plateau test results discussed in the previous section, in which the D_e values were independent of preheat temperatures. In theory, if the measurement protocol is suitable for dating the samples of interest, the doses obtained by the protocol (i.e., measured doses) should be identical to the given doses, making the ratio between the measured to given doses unity.

In the dose recovery experiments using the CW-OSL signals in both coarse and fine quartz grains (blue and black circles, respectively, in Fig. 6), the given doses for most samples were successfully recovered using the SAR protocol, the measured to given dose ratios (M/G ratio) being within ±10% of unity (Fig. 6). However, there was an exception for sample CAS72-2-1, where the measured dose underestimated the given dose by ~25% (for fine quartz), and incorporated significantly high uncertainty for the coarse quartz fraction. As indicated in the previous section (see section 4.1. Quartz CW-OSL Properties), the failure of sample CAS72-2-1 in the dose recovery test may be attributed to either the dim or slower nature of quartz OSL signals.

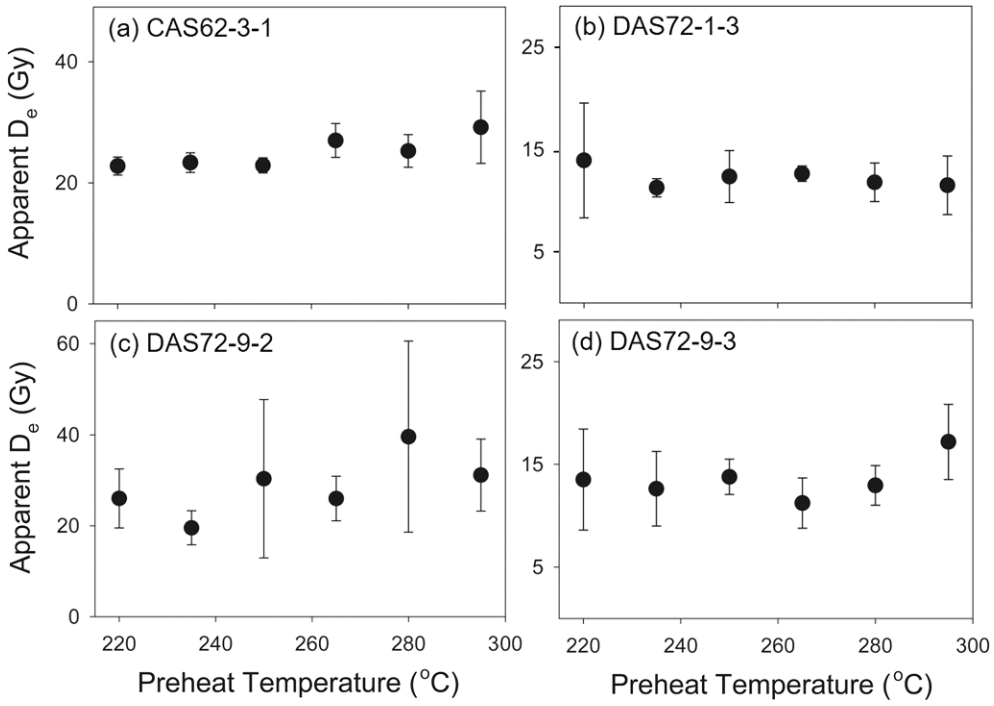

Fig. 5. Preheat plateau test using quartz (coarse) from palaeosol beneath (a) Cheoreum lava flow and (b–d) Darangsh scoria deposits. The D_e values are independent of preheat temperatures in the SAR protocol.

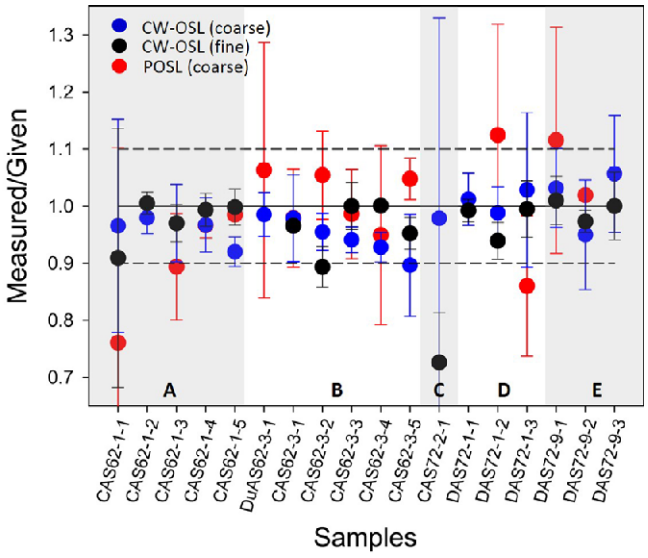

Fig. 6. Dose recovery test of SAR protocol using CW-OSL signals in coarse and fine quartz fractions and POSL signals in coarse quartz. The given doses for most sample accurately recovered, the measured/given dose ratios (M/G ratios) being within 10% of unity, with an exception of one sample from site C (CAS72-2-1). The doses measured by POSL signals are highly scattered with considerable uncertainties. However, the averaged M/G ratio for all the samples analyzed is 0.99 ± 0.10. Letters A–E denote the samples from sites A, B, C, D and E, respectively.

4.4. POSL Signal and Dose Recovery Test

Although the given doses were well recovered using the quartz CW-OSL signals applied to the SAR protocol, this does not guarantee the reliability in D_e estimation of the HF unetched coarse quartz samples (see section 3.1. OSL Dating); Even with the presence of K-rich feldspar contamination, the given doses can be accurately recovered, presumably due to the lack of time for the anomalous fading of trapped charges in K-rich feldspars. However, for natural samples, luminescence signals fade over geological time and even during laboratory storage, resulting in OSL age underestimation.

When the physical separation of K-rich feldspars from quartz is not possible, IR stimulation at an elevated temperature (IR wash), prior to every OSL signal measurement, may effectively remove the luminescence signals from feldspars (Wallinga et al., 2003; Roberts, 2007). However, for the HF unetched samples investigated here, a high temperature IR wash (at 125 °C for 100 s) did not seem to reduce the luminescence signals from feldspars down to a negligible level. As depicted in Figure 7 (blue lines), CW-OSL curves of dosed (26 Gy) coarse quartz grains from two HF unetched samples (CAS62-1-5 and CAS62-3-2), readout after an IR wash at 125 °C for 100 s, showed a significantly slow decay. It was therefore possible that a considerable amount of feldspar contamination was still contributing to the CW-OSL signals; Because the optical bleaching of feldspar is slower than for quartz (e.g., Godfrey-Smith et al., 1988), the CW-OSL signal from a mixture of quartz and feldspar decays more slowly than that of pure quartz. In fact, there are many other causes of the slow decay of quartz CW-OSL curves, for instance, the low power density of the stimulation light source, non-first order kinetics

https://doi.org/10.1007/s12303-019-0010-2

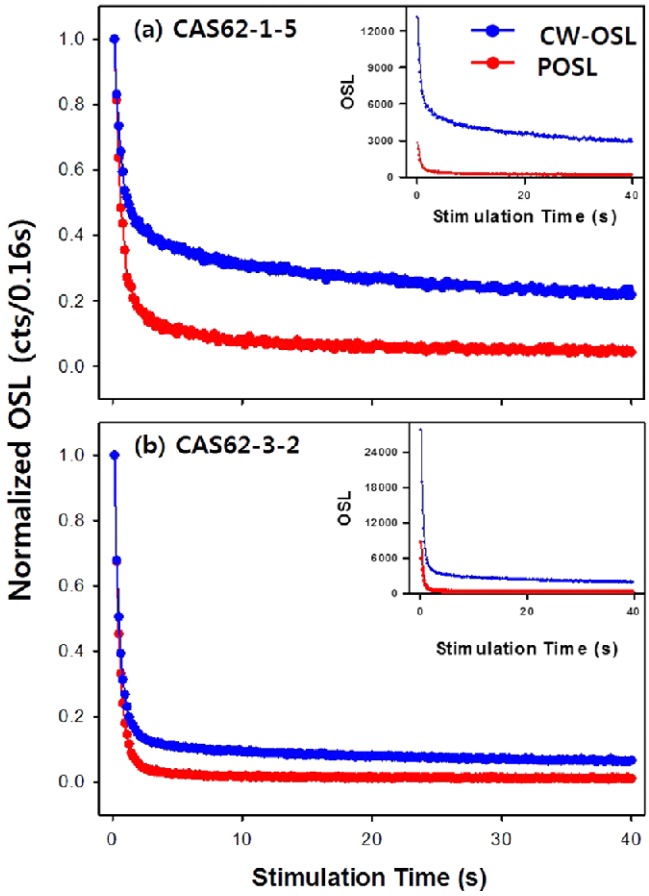

Fig. 7. Comparison of CW- and Pulsed OSL decay curves observed from HF-unetched samples from (a) site A and (b) site B. By pulsing the stimulation light source, the signal decay becomes much faster (red lines) than when stimulated by continuous-wave mode (blue lines). The signals were normalized to the initial count rates for comparison. In the insets shown are the decay curves without normalization.

(retrapping of charges) during the OSL signal production, significant contributions from non-fast OSL components, and so forth.

To examine whether the slow CW-OSL signal decay of the HF-unetched samples is the result of the imperfect removal of K-rich feldspars by applying the IR wash, we observed the POSL signals of the samples; It has been reported that, by stimulating a mixture of quartz and feldspars with pulsing mode, the signals from quartz and feldspars can be effectively separated because of the difference in *off*-time signal decay rates. The *off*-time signal of quartz decays much more slowly than that of K-rich feldspar (Denby et al., 2006; Tsukamoto and Rades, 2016). For this, the aliquots used to observe the CW-OSL signals described above were first β-dosed (26 Gy), preheated (at 260 °C for 10 s), and then IR washed (at 125 °C for 100 s). When measuring the POSL signals, the optimized *on*- and *off*-time combination to maximize the proportion of quartz signal can be sample-dependent. However, because the reader used in this study was not equipped with a photon timer, we could not perform experiments to determine the best *on*-and *off*-time combination for our samples. Instead, we adopted an *on*- and *off*-time of 50 μs as suggested by Ankjærgaard et al. (2010). The POSL signal decays obtained using only *off*-time signals from both samples are shown to be much faster than the conventional CW-OSL (red lines in Fig. 7), which indicates that the slow decay of the CW-OSL signals was at least partly due to the feldspar signal contamination and that pulsing the simulation light source following the IR wash was more effective for the separation of quartz signals, rather than using only a high temperature IR-wash.

Based on these observations, we investigated the possibility of applying POSL signals to dating the samples through dose recovery experiment. In this experiment, 54 coarse quartz aliquots from all the 18 samples (three aliquots per sample) were first optically bleached by blue-LEDs in the same manner as described in the previous section, and then given beta doses similar to the estimated D_e values of each sample. Then, the POSL SAR protocol, suggested by Ankjærgaard et al. (2010), was used to recover the given doses. The POSL SAR protocol consists of (1) irradiation of the main regeneration doses, (2) preheating at 260 °C for 10 s, (3) IR wash at 150 °C for 100 s, (4) POSL measurement at 125 °C for 80 s (*on*- and *off*-time of 50 μs), (5) test dose irradiation, (6) cut-heat to 220 °C for 0 s, (7) IR wash at 150 °C for 100 s, (8) POSL measurement at 125 °C for 80 s (*on*- and *off*-time of 50 μs) and (9) blue stimulation at an elevated temperature of 280 °C for 40 s (in CW-mode). For most samples, the measured doses are of large uncertainties (red symbols in Fig. 6). This is presumably due to poor counting statistics by losing *on*-time signals when measuring the POSL signals. In fact, from four of the samples (CAS62-1-2, CAS72-2-1, DAS72-1-1, and DAS72-9-3), we could not get a sufficient natural POSL signal count rate to calculate measured doses. In addition, even when measurable POSL signals were detected, the M/G ratios did not seem to be much improved and showed large uncertainties, compared with those obtained using conventional CW-OSL signals (Fig. 6). However, it should be noted here that the averaged M/G ratio obtained using the POSL signal is 0.99 ± 0.10, while those ratios by the conventional CW-OSL signals from both coarse and fine quartz are 0.97 ± 0.04 and 0.96 ± 0.07, respectively.

4.5. OSL Ages

As discussed in the previous sections, the CW-OSL SAR protocol was considered to be suitable for dating the samples investigated here. The POSL SAR protocol has been reported that it is potentially useful for dating samples which are suspected to include feldspar contamination (Dosseto et al., 2018) such as the HF unetched samples in this study. In this respect, although the given doses were not recovered as precisely as those using

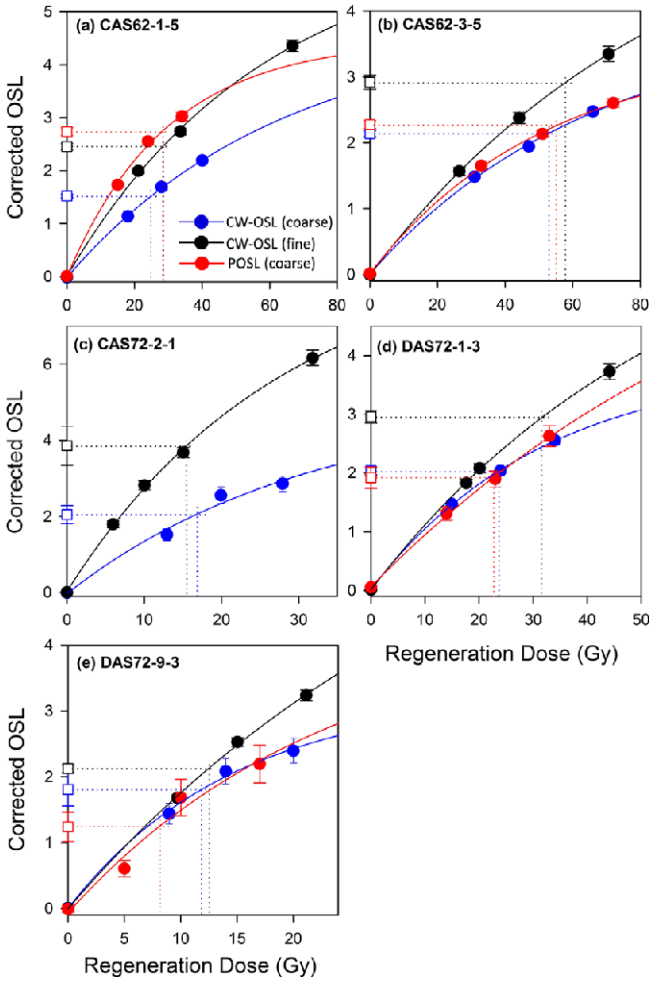

Fig. 8. Dose response growth curves (single saturating exponential functions) of CW-OSL signals and POSL signals using the lowermost (expected to be the oldest) samples from each site. For all the samples, the natural OSL signals are far less than the dose saturation level. For the sample from site C, POSL growth was not be constructed because of low POSL signal intensity, indistinguishable from background.

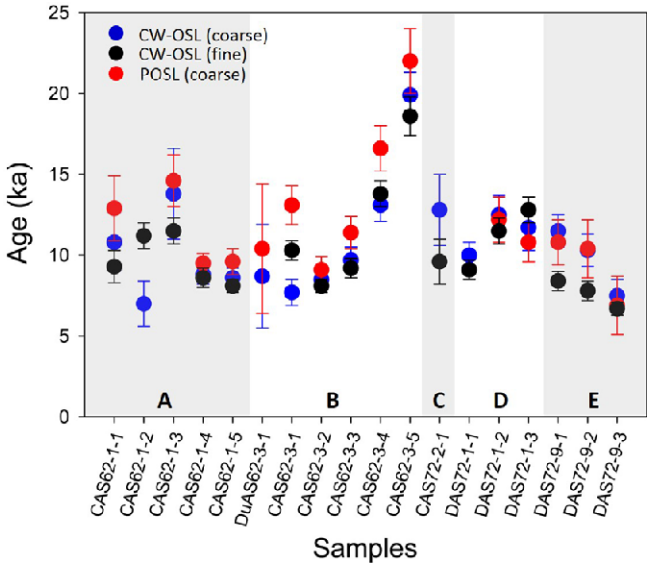

Fig. 9. The CW-OSL and POSL ages of the samples. The uncertainties are depicted in 2σ level (for more details, refer to the text). Letters A–E denote the samples from sites A, B, C, D and E, respectively.

CW-OSL signals in dose recovery experiments, we reckon that it is worth obtaining three different OSL ages from each sample (i.e., two CW-OSL SAR ages from the coarse and fine quartz fractions, and a POSL SAR age from the coarse quartz) and discuss them.

For D_e estimation of the samples, the same measurement conditions as those used in the dose recovery tests were used in the SAR protocol. OSL signals from multiple grain aliquots (both coarse and fine quartz; aliquot size of 8 mm) were used to build dose-response growth curves. In Figure 8, the CW-OSL and POSL growth curves of the lowermost (i.e., oldest) samples from each site are shown. For all of the samples, the D_e values were far lower than the $2D_0$ values of CW- and POSL growth curves, which indicate that the samples are without dose-saturation problems (Wintle and Murray, 2006). The CW-OSL signals from the fine quartz samples showed the most rapid growth with respect to the doses administered and the largest D_0 values (i.e., the highest saturation level). While the CW-OSL and the POSL signals from coarse quartz samples were observed to have similar growth properties, the measurement uncertainties were generally higher in POSL signals. In addition, as exemplified in Figure 8e, a considerable number of aliquots showed poorly defined POSL-SAR growth curves. These undesirable POSL signal properties for dating are presumably from the deteriorated counting statistics by losing the *on*-time signals as discussed earlier.

The OSL ages derived using CW- and Pulsed OSL signals are summarized in Table 1 and Figures 9 and 10. The CW-OSL ages beneath Cheoreum lava flow at sites A, B and C were in the range of 7–14 ka, 8–20 ka and 10–13 ka, respectively. The POSL ages of each sites were slightly older, but were still in the similar range (10–15 ka and 9–22 ka, for sites A and B, respectively). It should be noted here that the dose rates given in Table 1 are those derived from the palaeosol samples only. In theory, considering that gamma ray can travel as far as a few tens of centimeters (Aitken, 1998), it is desirable to take gamma contributions from the basaltic lavas into account when estimating dose rates of the samples if possible. However, physical modelling to understand the dose rate contributions from the overlying lavas is, in most cases, complicated and involves other sources of uncertainties which cannot be readily evaluated. Thus, in this study, we chose to calculate OSL ages using dose rates of the palaeosol samples only. The dry gamma dose rates of the Cheoreum and Dunjibong lavas are ~0.59 Gy/ka and ~0.76 Gy/ka, respectively, which are similar or

https://doi.org/10.1007/s12303-019-0010-2

Table 1. Equivalent doses, dosimetry and quartz OSL ages of the samples

Site	Sample[†]	Water Content[‡] (wt%)	Dry alpha[(a)] (Gy·ka^{-1})	Dry beta[(a)] (Gy·ka^{-1})	Dry gamma[(a)] (Gy·ka^{-1})	Dose rate[(b)] (Gy·ka^{-1})	coarse grain (CW-OSL)			fine grain (CW-OSL)			coarse grain (Pulsed-OSL)		
							D_e (Gy)	Age[(c)] (ka)	n[(d)]	D_e (Gy)	Age[(c)] (ka)	n[(d)]	D_e (Gy)	Age[(c)] (ka)	n[(d)]
A	CAS62-1-1	53	0.36 ± 0.01	1.09 ± 0.06	0.76 ± 0.03	1.26 ± 0.05	13.5 ± 1.0	10.8 ± 0.9	14	14.0 ± 0.6	9.3 ± 0.5	16	16.2 ± 1.0	12.9 ± 1.0	11
	CAS62-1-2	53	0.41 ± 0.01	1.16 ± 0.06	0.88 ± 0.03	1.37 ± 0.05	9.6 ± 0.9	7.0 ± 0.7	20	18.5 ± 0.4	11.2 ± 0.4	16	N.A.		
	CAS62-1-3	51	0.36 ± 0.01	1.05 ± 0.05	0.78 ± 0.02	1.26 ± 0.04	17.4 ± 1.6	13.8 ± 1.4	16	17.4 ± 0.3	11.5 ± 0.4	16	18.4 ± 0.8	14.6 ± 0.8	13
	CAS62-1-4	31	0.64 ± 0.02	2.14 ± 0.09	1.50 ± 0.04	2.78 ± 0.08	24.3 ± 0.7	8.8 ± 0.3	24	28.6 ± 0.5	8.6 ± 0.3	16	26.4 ± 0.6	9.5 ± 0.3	16
	CAS62-1-5	30	0.64 ± 0.02	2.24 ± 0.10	1.53 ± 0.04	2.91 ± 0.08	25.1 ± 0.6	8.6 ± 0.3	24	28.2 ± 0.5	8.1 ± 0.2	16	28.0 ± 0.8	9.6 ± 0.4	16
B	DuAS62-3-1	100	0.23 ± 0.20	1.04 ± 0.17	0.65 ± 0.31	0.89 ± 0.17	7.8 ± 0.2	8.7 ± 1.6	16	N.A.			9.3 ± 0.4	10.4 ± 2.0	8
	CAS62-3-1	65	0.61 ± 0.02	2.04 ± 0.09	1.35 ± 0.04	2.03 ± 0.06	15.6 ± 0.6	7.7 ± 0.4	18	25.0 ± 0.4	10.3 ± 0.3	16	26.7 ± 1.0	13.1 ± 0.6	14
	CAS62-3-2	34	0.60 ± 0.02	2.19 ± 0.10	1.45 ± 0.04	2.71 ± 0.08	22.9 ± 0.5	8.5 ± 0.3	24	26.0 ± 0.5	8.1 ± 0.2	16	24.7 ± 0.7	9.1 ± 0.4	16
	CAS62-3-3	33	0.61 ± 0.02	2.23 ± 0.09	1.45 ± 0.04	2.77 ± 0.08	27.0 ± 0.9	9.7 ± 0.4	24	30.4 ± 0.6	9.2 ± 0.3	16	31.5 ± 1.1	11.4 ± 0.5	16
	CAS62-3-4	29	0.63 ± 0.02	2.29 ± 0.10	1.52 ± 0.04	3.00 ± 0.08	38.9 ± 0.9	13.1 ± 0.5	24	48.6 ± 0.8	13.8 ± 0.4	16	49.1 ± 1.5	16.6 ± 0.7	16
	CAS62-3-5	44	0.64 ± 0.02	2.33 ± 0.10	1.53 ± 0.04	2.64 ± 0.07	52.7 ± 1.1	19.9 ± 0.7	24	58.4 ± 1.4	18.6 ± 0.6	16	58.1 ± 2.2	22.0 ± 1.0	15
C	CAS72-2-1	50	0.40 ± 0.02	1.12 ± 0.06	0.80 ± 0.03	1.33 ± 0.05	17.0 ± 1.4	12.8 ± 1.1	8	15.4 ± 1.0	9.6 ± 0.7	16	N.A.		
D	DAS72-1-1	61	0.48 ± 0.02	1.64 ± 0.07	1.13 ± 0.03	1.72 ± 0.05	17.3 ± 0.5	10.0 ± 0.4	24	18.7 ± 0.3	9.1 ± 0.3	16	N.A.		
	DAS72-1-2	75	0.51 ± 0.02	1.71 ± 0.08	1.18 ± 0.03	1.65 ± 0.05	20.6 ± 0.8	12.5 ± 0.6	24	22.7 ± 0.5	11.5 ± 0.4	16	20.2 ± 0.9	12.2 ± 0.7	16
	DAS72-1-3	52	0.55 ± 0.02	1.88 ± 0.09	1.28 ± 0.04	2.07 ± 0.06	24.1 ± 1.2	11.7 ± 0.7	24	31.6 ± 0.6	12.8 ± 0.4	16	22.4 ± 1.0	10.8 ± 0.6	13
E	DAS72-9-1	57	0.32 ± 0.01	1.09 ± 0.05	0.76 ± 0.02	1.23 ± 0.04	14.2 ± 0.5	11.5 ± 0.5	16	12.2 ± 0.4	8.4 ± 0.3	16	13.2 ± 0.7	10.8 ± 0.7	16
	DAS72-9-2	58	0.36 ± 0.01	1.19 ± 0.06	0.83 ± 0.02	1.31 ± 0.04	13.5 ± 0.5	10.3 ± 0.5	24	12.1 ± 0.2	7.8 ± 0.3	16	13.6 ± 0.1	10.4 ± 0.9	12
	DAS72-9-3	35	0.37 ± 0.01	1.22 ± 0.06	0.85 ± 0.03	1.58 ± 0.05	11.9 ± 0.7	7.5 ± 0.5	24	12.6 ± 0.3	6.7 ± 0.2	16	11.0 ± 1.4	6.9 ± 0.9	4

[†]The first letters of the sample codes indicate the monogenetic lava units overlying the samples (i.e., "C", "Du" and "D" refer to monogenetic volcanoes, "Cheoreum", "Dunjibong", and "Darangsh", respectively).
[‡]Present water content.
[(a)]Data from high-resolution low level gamma spectrometer were converted to infinite matrix dose rates using the conversion factors given in Olley et al. (1996). For alpha contribution, α value was assumed to be 0.03 (Mauz et al., 2006).
[(b)]The dose rates presented here are for coarse quartz grains and do not include alpha dose rates. The alpha dose rates were added to these values for the calculation of fine grain OSL ages. Contributions from cosmic rays were included using the equations given by Prescott and Hutton (1994).
[(c)]Central age ±1σ standard error.
[(d)]Number of aliquots used for statistical analysis.
N.A.: not analyzed due to insufficient amount of quartz grains for dating or low signal count rates.

slightly lower than those of the samples collected from just beneath the lavas (samples CAS62-1-1, DuAS62-3-1, and CAS62-3-1). Given these values, even if we assume that half of the gamma dose rates of the samples is attributed to the lavas, which is thought to be the maximum contribution, the final OSL ages of the samples should be affected by less than ~10%. Then, the gamma contributions from the lavas decrease exponentially and become negligible as the samples get away from them.

Of the samples collected from beneath Cheoreum lavas, sample CAS72-2-1 showed several unwanted OSL signal properties for dating; the initial CW-OSL signal count rates of this sample were less than ~700 cts (integrated counts in the initial 0.8 s) (Fig. 4) and the POSL signals were indistinguishable from background. In addition, it was not successful in the dose recovery experiment (Fig. 6). Therefore, it was considered that the OSL ages of this sample (both coarse and fine CW-OSL ages) should not be given credence. One sample collected from beneath Dunjibong lava flow (sample DuAS62-3-1, site B) was dated to be 8.7 ± 1.6 ka (CW-OSL, coarse quartz) and 10.4 ± 2.0 ka (POSL). The samples from sites D and E, which were collected from beneath Darangsh scoria deposits, showed the similar OSL ages, in the ranges of 9–13 ka and 7–12 ka, respectively. The ^{14}C ages derived from palaeosols at sites A, C, and E ranged between 10245 and 7440 Cal yr BP, which is broadly consistent with the OSL ages (Table 2).

However, with the exception of the samples from site B (from beneath Cheoreum lava flow), most of the OSL ages were stratigraphically inconsistent (Table 1 and Fig. 10). It is plausible that the moderate-to-low sensitivity of quartz from the palaeosols, as shown in Figure 4, leads to poor counting statistics when measuring OSL signals, resulting in inconsistent OSL ages. Alternatively, the quartz grains within the palaeosol profiles (20–60 cm in thickness, see section 2.2. Study Area and Sampling) might have been bioturbated enough for the OSL ages to be biased; Although we found lots of plant roots and burrowers (e.g., insects) within the profile, avoiding these bioturbation was not possible due to the limited thickness of each palaeosol profile. Nevertheless, from one profile where the OSL ages were stratigraphically consistent (Site B, beneath the Cheoreum lava flow), we could estimate a time-integrated sedimentation rate of ~0.05 mm/yr.

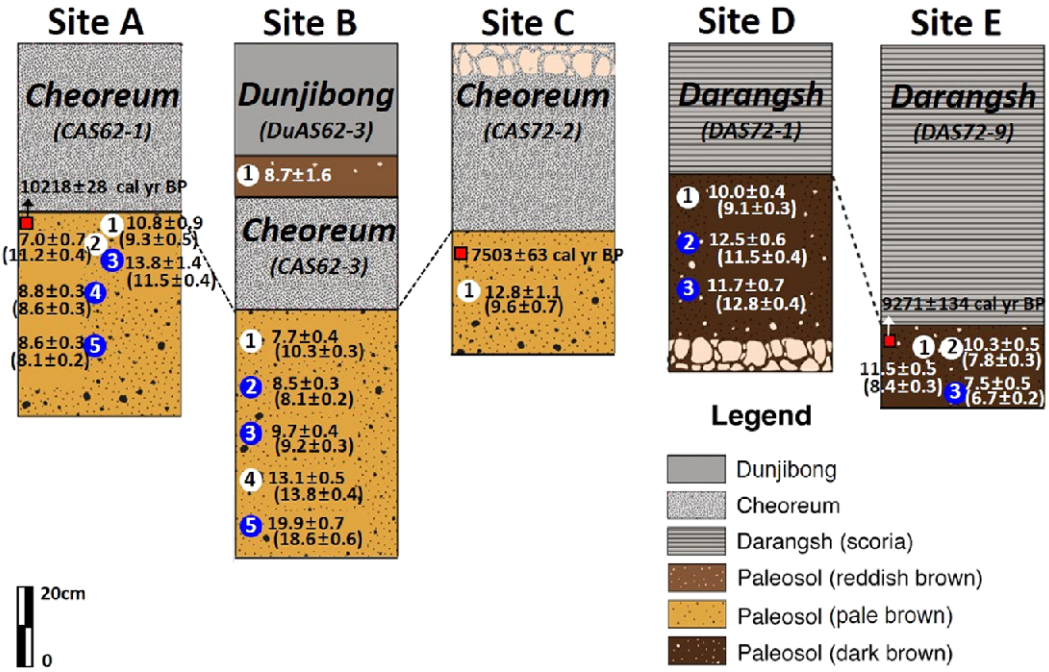

Fig. 10. Schematic columns of palaeosol profiles and the OSL ages of the samples in ka. Only CW-OSL ages are given here. OSL ages in parentheses are those obtained using fine quartz fractions. The samples shown as blue circles are those, all three ages ratios (two CW-OSL ages and POSL ages) of which are within 1.0 ± 0.1 at 2σ level. On the other hand, sample codes depicted with white circles are those, from which one of the three ages could not be derived or which have the age ratios out of 1.0 ± 0.1 interval at 2σ level.

Table 2. ^{14}C ages of the samples

Site	Sample	^{14}C age[(a)] (yr BP)	Calibrated ^{14}C age[(a)] (Cal yr BP)	Note
A	CAS62-1-C1	9050 ± 30	10218 ± 28	Palaeosol
C	CAS72-2-C1	6610 ± 30	7503 ± 63	Palaeosol
E	DAS72-9-C1	8280 ± 30	9271 ± 134	Palaeosol

[(a)]Uncertainties are given in 2σ standard errors.

In Figure 11, three sets of OSL ages (CW-OSL ages from coarse and fine quartz and the POSL ages) are compared with one another. For the samples from sites A and B, the POSL ages were generally higher than the CW-OSL ages of both coarse and fine quartz grains. Unexpectedly, it appears to be difficult to argue that the CW-OSL ages of the HF unetched samples were significantly affected by feldspar contaminations, because the POSL ages were almost identical to the CW-OSL ages of the HF-unetched samples, when taking the uncertainties in 2σ level (Figs. 9 and 11a); The age differences are only ~7–25% (14% on average; samples CAS62-1-4, CAS62-1-5, CAS62-3-2, CAS62-3-3, CAS62-3-4, and CAS62-3-5). However, despite the POSL signals measured after the IR wash being observed to be effective for minimizing the contributions from feldspar contamination (Fig. 7), a comparison of the POSL ages with the CW-OSL ages should still be interpreted cautiously, due to the poor counting statistics in natural POSL signals as mentioned earlier. Particularly, the POSL dating solely should not be the method of choice for dating dim samples such as those investigated here (e.g., for samples with initial natural CW-OSL count rates less than ~1000 cts/0.16s).

It is interesting to notice that, nine samples, out of eighteen analysed, are of the age ratios within 1.0 ± 0.1 at 2σ level (for all three age ratios in Fig. 11); These are samples CAS62-1-3, CAS62-1-4, and CAS62-1-5(Site A), CAS62-3-2, CAS62-3-3, and CAS62-3-5 (Site B), DAS72-1-2 and DAS72-1-3 (Site D), and DAS72-9-3 (Site E). The OSL ages of these samples were ~8–15 ka (Site A), ~8–22 ka (Site B), ~10–13 ka (Site D) and ~7–8 ka (Site E). The OSL ages of these samples taken as the most reliable ones in this study, it appears that Cheoreum lava and Darangsh scoria deposits have formed during the Early Holocene period (after ~7–8 ka). Although the OSL age of the palaeosol beneath Dunjibong lava flow has not been well defined here (i.e., no CW-OSL age for fine grains and inconsistent CW-OSL and POSL ages for coarse grains), the age of the sample (DuAS62-3-1, ~9 ka) was indistinguishable from the ages beneath Cheoreum lava flow at Site B. Thus, we consider that Dunjibong lava flow have formed immediately after the eruption of Cheoreum unit.

https://doi.org/10.1007/s12303-019-0010-2

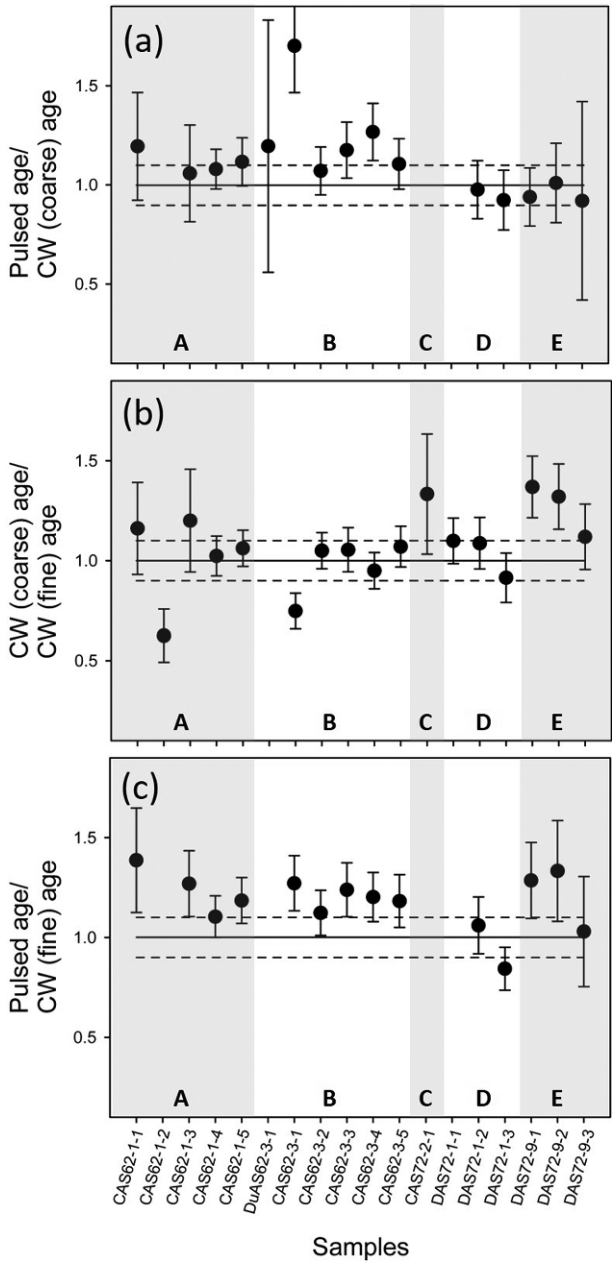

Fig. 11. Comparison of OSL ages by using CW-OSL signals in coarse and fine quartz fractions, and POSL signals ((a) POSL age vs. CW-OSL (coarse) age, (b) CW-OSL (coarse) age vs. CW-OSL (fine) age, (c) POSL age vs. CW-OSL (fine) age). The uncertainties are depicted at 2σ level. Letters A–E denote the samples from sites A, B, C, D and E, respectively.

5. CONCLUSIONS

Quartz extracts from the palaeosols beneath lava flows and scoria deposits, ejected from three monogenetic volcanoes in northeastern Jeju Island (Cheoreum, Dunjibong and Darangsh) exhibited moderate-to-dim OSL signal sensitivities. For most samples investigated in this study, however, the doses given in the laboratory were accurately recovered by the SAR protocol with no dependency of quartz equivalent dose values on measurement conditions (e.g., preheating etc.), which indicated that the protocol was suitable for dating the samples.

POSL signals were shown to be effective to separate quartz OSL signals from a mixture of quartz and K-rich feldspars. However, presumably due to deteriorated counting statistics, dating with the POSL signal alone is not considered to be the method of choice, particularly for dim samples.

The OSL ages, based on CW-OSL signals in the coarse and fine quartz fractions, were ranging 19.9–7.0 and 18.6–6.7 ka, respectively, which was consistent with ^{14}C dating results. Further, from one of the palaeosol profiles covered by Cheoreum, an averaged sedimentation rate of ~0.05 mm/yr could be estimated. Conclusively, the OSL ages of the palaeosols intercalated with lavas and scoria deposits infer that the northeastern part of Jeju Island has been volcanically active during the Early Holocene (after ~7 ka), supporting the previous views regarding volcanism in this island.

ACKNOWLEDGMENTS

This work was supported by the National Research Foundation of Korea Grants funded by the Korean Government (MSICT) (2018, R&D Equipment Engineer Education Program, 2014R1A6A9064166 and 2016R1A2B4007283), and a Korea Basic Science Institute grant (C38709).

REFERENCES

Ahn, U.S., 2016, Study of the last volcanic activity on historical records on Jeju Island, Korea. Journal of the Petrological Society of Korea, 25, 69–83. (in Korean with English abstract)

Ahn, U.S. and Hong, S.S., 2017, Volcanological history of the Baengnokdam summit crater area, Mt. Halla, Jeju Island, Korea. Journal of the Petrological Society of Korea, 26, 221–234. (in Korean with English abstract)

Ahn, U.S., Choi, J.H., and Yeo, E.Y., 2017, Eruption timing of the Geomun Oreum through the comparison of radiocarbon and quartz OSL ages. Journal of the Geological Society of Korea, 53, 367–376. (in Korean with English abstract)

Aitken, M.J., 1985, Thermoluminescence Dating. Academic Press, London, 359 p.

Aitken, M.J., 1998, An Introduction to Optical Dating. Oxford University Press, Oxford, 267 p.

Ankjærgaard, C., Jain, M., Thomsen, K.J., and Murray, A.S., 2010, Optimising the separation of quartz and feldspar optically stimulated luminescence using pulsed excitation. Radiation Measurements, 45, 778–785.

Bonde, A., Murray, A.S., and Friedrich, W.L., 2001, Santorini: luminescence dating of a volcanic province using quartz? Quaternary Science Reviews, 20, 789–793.

Brenna, M., Cronin, S.J., Smith, I.E.M., Maas, R., and Sohn, Y.K., 2012a,

How small-volume basaltic magmatic systems develop: a case study from the Jeju Island volcanic field, Korea. Journal of Petrology, 53, 985–1018.

Brenna, M., Cronin, S.J., Smith, I.E.M., Sohn, Y.K., and Maas, R., 2012b, Spatio-temporal evolution of a dispersed magmatic system and its implications for volcano growth, Jeju Island volcanic field, Korea. Lithos, 148, 337–352.

Brenna, M., Cronin, S.J., Kereszturi, G., Sohn, Y.K., Smith, I.E.M., and Wijbrans, J., 2015, Intraplate volcanism influenced by distal subduction tectonics at Jeju Island, Republic of Korea. Bulletin of Volcanology, 77, 7. https://doi.org/10.1007/s00445-014-0896-5

Bronk Ramsey, C., 2009, Bayesian analysis of radiocarbon dates. Radiocarbon, 51, 337–360.

Cheong, C.S., Choi, J.H., Sohn, Y.K., Kim, J.C., and Jeong, G.Y., 2007, Optical dating of hydromagmatic volcanoes on the southwestern coast of Jeju Island, Korea. Quaternary Geochronology, 2, 266–271.

Choi, J.H., Duller, G.A.T., Wintle, A.G., and Cheong, C.S., 2006, Luminescence characteristics of quartz from the Southern Kenyan Rift Valley: dose estimation using LM-OSL SAR. Radiation Measurements, 41, 847–854.

Denby, P.M., Bøtter-Jensen, L., Murray, A.S., Thomsen, K.J., and Moska, P., 2006, Application of pulsed OSL to the separation of the luminescence components from a mixed quartz/feldspar sample. Radiation Measurements, 41, 774–779.

Dosseto, A., May, J.-H., Choi, J.H., Swander, Z.J., Fink, D., Korup, O., Hesse, P., Singh, T., Mifsud, C., and Srivastava, P., 2018, Late Quaternary fluvial incision and aggradation in the Lesser Himalaya, India. Quaternary Science Reviews, 197, 112–128.

Esser, R.P., McIntosh, W.C., Heizler, M.T., and Kyle, P.R., 1997, Excess argon in melt inclusions in zero-age anorthoclase feldspar from Mt. Erebus, Antarctica, as revealed by the $^{40}Ar^{39}Ar$ method. Geochimica et Cosmochimica Acta, 61, 3789–3801.

Fuchs, M., Kreutzer, S., Fischer, M., Sauer, D., and Sørensen, R., 2012, OSL and IRSL dating of raised beach sand deposits along the southeastern coast of Norway. Quaternary Geochronology, 10, 195–200.

Gliganic, L.A., Meyer, M.C., Sohbati, R., and Barrett, S., 2019, OSL surface exposure dating of a lithic quarry in Tibet: laboratory validation and application. Quaternary Geochronology, 49, 199–204.

Godfrey-Smith, D.I., Huntley, D.J., and Chen, W.H., 1988, Optical dating studies of quartz and feldspar sediment extracts. Quaternary Science Reviews, 7, 373–380.

Jenkins, G.T.H., Duller, G.A.T., Roberts, H.M., Chiverrell, R.C., and Glasser, N.F., 2018, A new approach for luminescence dating glaciofluvial deposits – high precision optical dating of cobbles. Quaternary Science Reviews, 192, 263–273.

Koh, G.W., Park, J.B., Kang, B.R., Kim, G.P., and Moon, D.C., 2013, Volcanism in Jeju Island. Journal of the Geological Society of Korea, 49, 209–230. (in Korean with English abstract)

Koh, J.S., Yun, S.H., and Kang, S.S., 2003, Petrology of the volcanic rocks in the Paekrogdam Crater area, Mt. Halla, Jeju Island. Journal of the Petrological Society of Korea, 12, 1–15. (in Korean with English abstract)

Lee, J.Y., Kim, J.C., Park, J.B., Lim, J.S., Hong, S.S., and Choi, H., 2014, Age of volcanic activity from Quaternary deposits in Sangchang-ri, Jeju island, Korea. Journal of the Geological Society of Korea, 50, 697–706. (in Korean with English abstract)

Lee, K. and Yang, W.S., 2006, Historical seismicity of Korea. Bulletin of the Seismological Society of America, 96, 846–855.

Li, B., Jacobs, Z., Roberts, R.G., and Li, S.H., 2013, Extending the age limit of luminescence dating using the dose-dependent sensitivity of MET-pIRIR signals from K-feldspar. Quaternary Geochronology, 17, 55–67.

Mauz, B., Packman, S., and Lang, A., 2006, The alpha effectiveness in silt-sized quartz: new data obtained by single and multiple aliquot protocols. Ancient TL, 24, 47–52.

Murray, A.S. and Wintle, A.G., 2000, Luminescence dating of quartz using an improved single-aliquot regenerative-dose protocol. Radiation Measurements, 32, 57–73.

Murray, A.S. and Wintle, A.G., 2003, The single aliquot regenerative dose protocol: potential for improvements in reliability. Radiation Measurements, 37, 377–381.

Nakamura, E., Campbell, I.H., McCulloch, M.T., and Sun, S.S., 1989, Chemical geodynamics in a back arc region around the Sea of Japan: implications for the genesis of alkaline basalts in Japan, Korea and China. Journal of Geophysical Research: Solid Earth, 94, 4634–4654.

Ramos, F.C., Heizler, M.T., Buettner, J.E., Gill, J.B., Wei, H.Q., Dimond, C.A., and Scott, S.R., 2016, U-series and $^{40}Ar/^{39}Ar$ ages of Holocene volcanic rocks at Changbaishan volcano, China. Geology, 44, 511–514.

Reimer, P.J., Bard, E., Bayliss, A., Beck, J.W., Blackwell, P.G., Bronk Ramsey, C., Buck, C.E., Cheng, H., Edwards, R.L., Friedrich, M., Grootes, P.M., Guilderson, T.P., Haflidason, H., Hajdas, I., Hatté, C., Heaton, T.J., Hoffmann, D.L., Hogg, A.G., Hughen, K.A., Kaiser, K.F., Kromer, B., Manning, S.W., Niu, M., Reimer, R.W., Richards, D.A., Scott, E.M., Southon, J.R., Staff, R.A., Turney, C.S.M., and van der Plicht, J., 2013, IntCal13 and Marine13 radiocarbon age calibration curves 0–50,000 years cal BP. Radiocarbon, 55, 1869–1887.

Roberts, H.M., 2007, Assessing the effectiveness of the double-SAR protocol in isolating a luminescence signal dominated by quartz. Radiation Measurements, 42, 1627–1636.

Sohbati, R., Murray, A.S., Porat, N., Jain, M., and Avner, U., 2015, Age of a prehistoric "Rodedian" cult site constrained by sediment and rock surface luminescence dating techniques. Quaternary Geochronology, 30, 90–99.

Sohn, Y.K. and Park, K.H., 2004, Early-stage volcanism and sedimentation of Jeju Island revealed by the Sagye borehole, SW Jeju Island, Korea. Geosciences Journal, 8, 73–84.

Sohn, Y.K., Park, J.B., Khim, B.K., Park, K.H., and Koh, G.W., 2002, Stratigraphy, petrochemistry and Quaternary depositional record of the Songaksan tuff ring, Jeju Island, Korea. Journal of Volcanology and Geothermal Research, 119, 1–20.

Sun, X., Yi, S., Lu, H., and Zhang, W., 2017, TT-OSL and post-IR IRSL dating of the Dali Man site in central China. Quaternary International, 434, 99–106.

Tatsumi, Y., Shukuno, H., Yoshikawa, M., Chang, Q., Sato, K., and Lee, M.W., 2005, The petrology and geochemistry of volcanic rocks on Jeju Island: plume magmatism along the Asian continental margin. Journal of Petrology, 46, 523–553.

Tsukamoto, S. and Rades, E.F., 2016, Performance of pulsed OSL stimulation for minimising the feldspar signal contamination in quartz samples. Radiation Measurements, 84, 26–33.

Tsukamoto, S., Rink, W.J., and Watanuki, T., 2003, OSL of tephric loess and volcanic quartz in Japan and an alternative procedure for estimating D_e from a fast OSL component. Radiation Measurements, 37, 459–465.

Tsukamoto, S., Duller, G.A.T., Wintle, A.G., and Muhs, D., 2011, Assessing the potential for luminescence dating of basalts. Quaternary Geochronology, 6, 61–70.

Thiel, C., Buylaert, J.-P., Murray, A.S., Elmejdoub, N., and Jedoui, Y., 2012, A comparison of TT-OSL and post-IR IRSL dating of coastal deposits on Cap Bon peninsula, north-eastern Tunisia. Quaternary Geochronology, 10, 209–217.

Wallinga, J., Murray, A.S., and Bøtter-Jensen, L., 2003, Measurement of the dose in quartz in the presence of feldspar contamination. Radiation Protection Dosimetry, 101, 367–370.

Wintle, A.G. and Murray, A.S., 2006, A review of quartz optically stimulated luminescence characteristics and their relevance in single-aliquot regeneration dating protocols. Radiation Measurements, 41, 369–391.